J. Fluid Mech. (1985), *vol.* 152, *pp.* 83–111
Printed in Great Britain

Far-field noise of a subsonic jet under controlled excitation

By K. B. M. Q. ZAMAN
NASA-Langley Research Center, Hampton, Virginia 23665, U.S.A.

The phenomena of excitation-induced suppression and amplification of broadband jet noise have been experimentally investigated in an effort to understand the mechanisms, especially in relation to the near flow-field large-scale structure dynamics. Suppression is found to occur only in jets at low speeds with laminar exit boundary layers, the optimum occurring for excitation at $St_\theta \approx 0.017$, where St_θ is the Strouhal number based on the initial shear-layer momentum thickness. The suppression mechanism is linked to an initial-condition effect on the large-scale structure dynamics. The interaction and evolution of laminar-like structures at low jet speeds produce more (normalized) noise and turbulence, compared to asymptotically lower levels at high speeds when the initial shear layer is no longer laminar. The effect of initial condition has been demonstrated by tripped versus untripped jet data. The excitation at $St_\theta \approx 0.017$ results in a quick roll-up and transition of the laminar shear-layer vortices, yielding coherent structures which are similar to those at high speeds. Thus, the broadband noise and turbulence are suppressed, but at the most to the asymptotically lower levels. When at the asymptotic level, the broadband jet noise can only be amplified by the excitation; the amplification is found to be maximum for excitation in the St_D range of 0.65–0.85, St_D being the Strouhal number based on the jet diameter. Excitation in this St_D range also produces strongest vortex-pairing activity. From spectral analysis of the flow-field and the near sound-pressure field, it is inferred that the pairing process induced by the excitation is at the origin of the broadband noise amplification.

1. Introduction

Accumulated experimental evidence makes it abundantly clear that the near flow-field of an axisymmetric jet is dominated by large-scale, coherent, vortical structures (e.g. Lau, Fisher & Fuchs 1972; Browand & Laufer 1975; Davies & Yule 1975; Moore 1977; Zaman & Hussain 1984). It is also clear that one can significantly alter these structures by artificial excitation (e.g. Crow & Champagne 1971; Chan 1974; Ho & Huang 1982; Richarz 1983; Zaman & Hussain 1980). The effect of excitation on the radiated jet noise has also been explored in a number of experiments (e.g. Bechert & Pfizenmaier 1975; Moore 1977; Kibens 1980) but relatively little is known about the link between observed noise modification under excitation and the corresponding altered states of the coherent structures. The present experimental investigation is an effort to obtain a better grasp of this link, through a study of the noise and coherent structure modification, by means of controlled excitation. Two principal influences on the far-field noise are addressed: broadband noise amplification and suppression.

The broadband jet noise amplification phenomenon was first observed independently by Bechert & Pfizenmaier (1975) and by Moore (1977). Subsequently, it has been observed and studied (including analytical modelling) by several other investigators

(e.g. Deneuville & Jacques 1977; Ffowcs Williams & Kempton 1978; Jubelin 1980; Crighton 1981; Ahuja *et al.* 1982). The noise amplification is a curious phenomenon in which excitation imparted at the jet exit, in the form of a plane or higher-order mode tone, results in an increase in the broadband energy of the far-field noise. The amplification is quite uniform in frequency as well as in directivity; thus the amplified noise appears 'morphologically similar to ordinary jet noise but the sound levels are higher' (Deneuville & Jacques 1977). Besides being of profound academic interest, this phenomenon also had far-reaching implications for the 'excess' or 'internal' noise from practical as well as model jets. The erstwhile illusive 'internal noise' became reconcilable or even explainable in terms of jet excitation by background noise fields (Crighton 1981). Academically, the phenomenon is profound because it lends a handle to the experimentalist (and also to the theoretician) by which jet noise could be manipulated, with a grasp on the cause and effect, thus allowing a probe into the noise-producing mechanism.

Excitation has also been observed to yield a rather intriguing broadband jet noise suppression, typically at low Reynolds numbers (Kibens 1980; Morrison & McLaughlin 1979). A related and remarkable phenomenon of turbulence suppression, first reported by Vlasov & Ginevskiy (1974), was studied in detail by Zaman & Hussain (1981). By excitation at $St_\theta \approx 0.017$, not only the broadband but the total turbulence could be reduced over the entire near flow-field ranging over $1 \lesssim x/D \lesssim 8$. The provocative question that remained unanswered was, could such excitation lead to a practical jet noise suppression method?

A summary of previous experiments reporting amplification/suppression of broadband noise/turbulence was given by Crighton (1981). He made the curious observation that a Reynolds number (Re_D) of about 10^5 appeared to be a barrier below and above which artificial excitation resulted in the suppression and the amplification, respectively. Such an Re_D dependence was intriguing, conflicted with similarity laws, and remained to be demonstrated in 'a set of experiments on the same rig'. These questions are addressed in the present experiment.

The motivation for the present study stemmed partly from the investigations on the large-scale coherent structure dynamics, carried out by Hussain & Zaman, hereinafter referred to as HZ, (1980, 1981), and Zaman & Hussain, hereinafter referred to as ZH, (1980, 1981, 1984). A précis of these works relating to the present investigation is given below.

The evolution and characteristics of the 'preferred mode' coherent structure have been documented with and without controlled excitation (HZ 1981, ZH 1984). The structure characteristics were educed by conditional- or phase-averaging, using a velocity signal from the flow as reference. The 'coherent' properties associated with these structures not only accounted for a significant part of the Reynolds stress etc. but also organized the 'incoherent' turbulence; e.g. the location of peak coherent vorticity determined the 'saddle point' in the 'incoherent Reynolds stress' distribution (HZ, 1980, 1981). The 'braid' region between coherent structures has been identified as playing a key role in turbulence production (see Hussain 1983). The axisymmetric coherent structures, induced under the plane-wave excitation, could be detected as far downstream as $x/D \approx 6$ (HZ 1981); the structures in the natural jet were found to be primarily of the axisymmetric mode, and also independent of Re_D measured up to $Re_D \approx 10^6$. The excitation-induced structure agrees well with the natural structure for small amplitudes of excitation, but higher amplitudes yield significantly stronger structures, marked by higher core vorticity (ZH 1984). The turbulence suppression phenomenon, mentioned above, occurs for the 'shear-layer mode' of

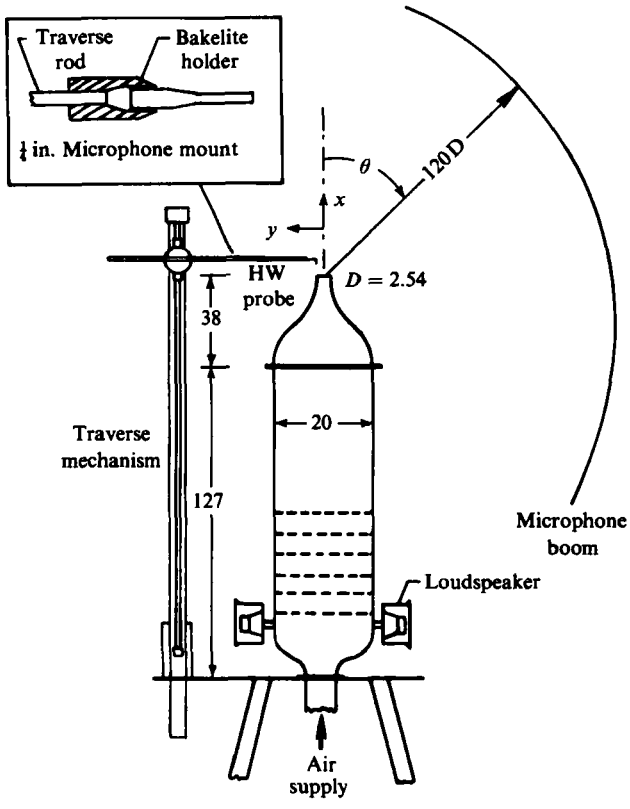

FIGURE 1. Schematic diagram of the experimental facility. Dimensions are in cm.

excitation, while excitation at appropriate 'jet column mode' Strouhal number (St_D) induces strong pairing activity of the structures (HZ 1980, ZH 1980). These two effects, which are pivotally connected with the noise suppression/amplification, will be described in detail in the text.

The above knowledge of the coherent-structure dynamics and of the multi-faceted effects of controlled excitation formed a vantage point from which the present study was attempted. The objective has been to determine the parameters controlling the broadband jet noise amplification/suppression, relate observed effects on the noise and the large-scale structures, and thus understand the role of these structures in the noise modification and in jet noise production mechanisms in general.

2. Experimental facility

2.1. *Flow facility and procedures*

The experiments were carried out in a 9.1 m × 6.1 m × 7.6 m anechoic chamber. The jet flow was obtained by passing compressed air through an upright, 20 cm diameter, cylindrical settling chamber. The flow finally passed through a contoured, convergent nozzle which gradually ended into a short cylindrical section of diameter $D = 2.54$ cm. A schematic diagram of the flow facility is shown in figure 1. A small (DISA) traverse mechanism mounted on a vertical traverse mechanism was used to make flow-field and near-sound-field measurements. For all far-field noise data reported here, the height of the vertical traverse mechanism was adjusted to a minimum so that the

small one could only draw a probe in and out of the flow to monitor the boundary-layer characteristics, excitation level, etc. Near-field sound (in the vicinity of the jet edge) was measured by a $\frac{1}{4}$ in. (B & K) microphone. The far-field noise was measured by $\frac{1}{2}$ in. (B & K) microphones held fixed on an arc of a circle at a distance $R/D = 120$ from the jet exit centre. (The probe traverse plane was perpendicular to the microphone boom plane, although the two are shown to coincide in figure 1 for convenience.) Standard constant-temperature anemometry was used for flow measurements. Noise and velocity spectra were obtained by a spectrum analyser (Spectral Dynamics SD360). The controlled excitation to the jet was imparted by means of two loudspeakers attached to the side of the settling chamber, both driven in phase by the same signal. The purpose of using two speakers was to obtain higher excitation amplitude. All data acquisition, probe traverse, etc. were done under remote computer control (PDP 1170) from an adjacent 'control room' which housed all the instrumentation.

2.2. *Characteristics of the flow facility*

Top-hat mean velocity profiles with thin boundary layers were obtained at the exit of the jet at all speeds (U_e). The longitudinal mean (U) and r.m.s. (u') velocity profiles in the exit boundary layer, measured about 0.5 mm downstream of the exit plane, are shown in figure 2(a) for three U_e. The mean velocity profiles agreed with the laminar flat-plate Blasius profile at all U_e. The turbulence intensity in the core of the jet at the exit plane was less than 0.3% of U_e. However, the fluctuation intensity in the boundary layer rapidly increased above a Reynolds number ($Re_D = U_e D/\nu$) of about 10^5. The variations of the maximum fluctuation (u'_{max}) and the momentum thickness (Θ) with Re_D and Mach number ($M = U_e/a_0$, a_0 being the ambient sound speed) are shown in figure 2(b). Thus, based on the U-profile and u'_{max} data, the exit boundary layer can be characterized as 'fully laminar' below $Re_D \approx 10^5$, but only 'nominally laminar' above this Re_D, becoming 'nominally turbulent' for $Re_D \lesssim 2.5 \times 10^5$. (Between the asymptotic 'fully laminar' and 'fully turbulent' states, the exit boundary layer can be transitional; this is, in fact, the state encountered in most model jets. The transitional state can again be divided into two categories: 'nominally laminar' and 'nominally turbulent' as in the discussion by Hussain 1980.)

The resonance characteristics of the jet rig–loudspeaker combination are shown in figure 3 for a jet speed of $U_e = 43$ m s^{-1}, measured while keeping the voltage across the voice-coil of a loudspeaker constant and varying the frequency (f_p) in discrete steps. Figure 3(a) shows the filtered r.m.s. velocity fluctuation at the driving frequency, measured at the exit plane (u'_{fe}) at $y = 0.25D$. Figure 3(b) shows the sound intensity at the exit plane (L_e, dB re 2×10^{-5} N/m^2), measured by a $\frac{1}{8}$ in. microphone fitted with a (B & K) 'nose cone' and placed at $y = -0.25D$. Note that the 'pseudo sound', due to the (low) turbulence intensity, appearing in L_e is negligible. Figure 3(c) shows the far-field sound intensity (L) at $\theta = 90°$, measured simultaneously with u'_{fe} and L_e. All three quantities, as well as L at $\theta = 30°$ (not shown), show the same resonance frequencies. Measurements with no flow also showed similar variations of L_e and L to those in figures 3(b,c). The first peak at $f_p \approx 120$ Hz represents the half-wave resonance based on the settling-chamber length; resonance at the next three harmonics of this f_p are also prominent. Note that the u'_{fe} peaks have higher amplitudes at the lower frequencies while large-amplitude L_e occurred over a higher f_p range. One observes that the high-amplitude L_e occurs in a range of f_p bounded by the cut-on frequency (for higher-order mode waves) based on the jet diameter (about 8 kHz) and that based on the settling-chamber diameter (about 1 kHz).

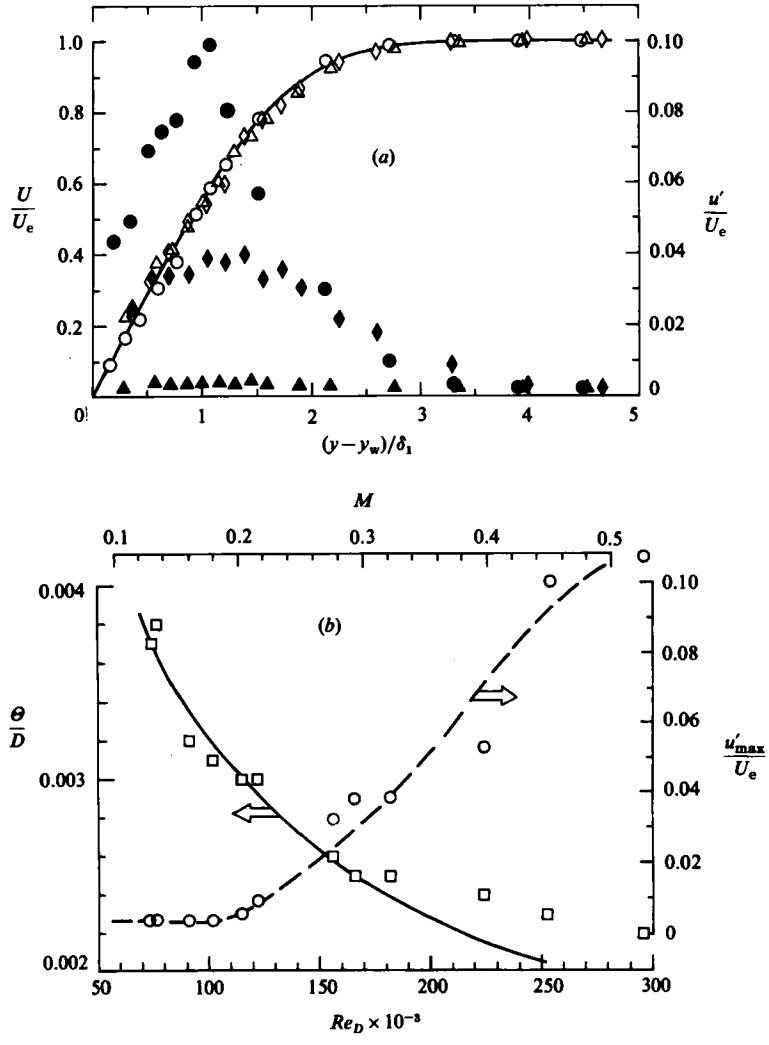

FIGURE 2. (*a*) Profiles of the longitudinal mean velocity (U) and r.m.s. fluctuation intensity (u') in the exit boundary layer; y_w is location of nozzle wall, δ_1 is displacement thickness. △, $U_e = 60$ m s^{-1}; ◇, $U_e = 97$ m s^{-1}; ○, $U_e = 148$ m s^{-1}. Solid line represents Blasius profile; open symbols for U, solid symbols for u'. (*b*) Variations of exit boundary-layer momentum thickness (square symbols), and maximum fluctuation intensity (circles), as a function of Re_D and M.

Additional higher-order mode waves are cut on inside the chamber but are cut off by the nozzle in this range. Whether this would explain the observed trend is not clear and the matter was considered beyond the scope of the present study.

The question arose as to which one of u'_{te}/U_e and L_e is a more meaningful parameter for monitoring the excitation level. Note that the parameter u'_{te}/U_e approximates the relative vorticity perturbation in the shear layer, while L_e, representing mean square pressure fluctuation, approximates the momentum perturbation at the jet exit. Typically, u'_{te}/U_e has been used in the large-scale coherent-structure studies (e.g. Crow & Champagne 1971; ZH 1980). Either of u'_{te}/U_e or L_e has been used in instability and aeroacoustics studies (e.g. u'_{te}/U_e by Bechert & Pfizenmaier 1975; L_e by Chan 1974, Moore 1977; Ahuja *et al.* 1982). However, a cross-reference between

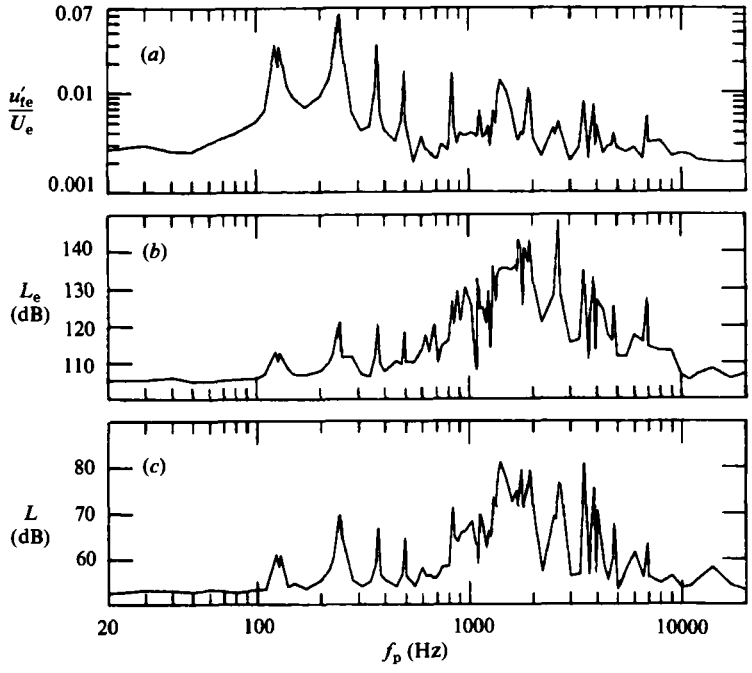

FIGURE 3. Resonance characteristics of the flow facility. (*a*) Filtered r.m.s. velocity fluctuation, u'_{fe}/U_e at jet exit, (*b*) sound-pressure level, L_e(dB) at jet exit, and (*c*) sound-pressure level in the far field at $\theta = 90°$. Data obtained by varying f_p while keeping voltage to loudspeaker input constant.

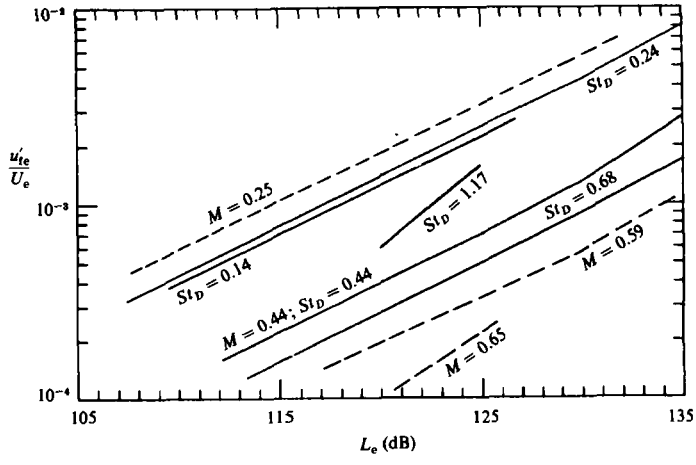

FIGURE 4. Variation of u'_{fe}/U_e with L_e; $M = 0.44$ for solid lines, $St_D = 0.44$ for dashed lines.

the two has not been provided in any of these studies, nor has the significance of each been discussed. An effort was made to relate the two over the parameter ranges covered in the present study.

Variations of u'_{fe}/U_e with L_e are shown in figure 4. Each curve was obtained by varying the power input to the loudspeaker for fixed M and St_D. One set of curves was obtained with $St_D = 0.44$ but for different M; the other set was obtained with $M = 0.44$, but for different St_D. The slopes of these curves confirm that u'^2_{fe} is

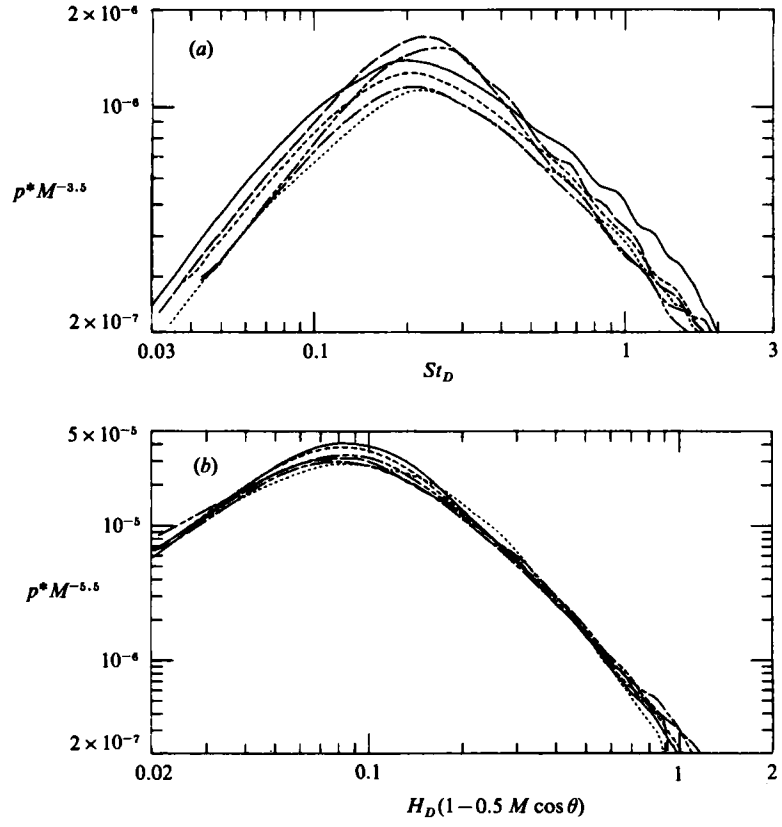

FIGURE 5. Power spectral density (PSD) of far-field noise for (*a*) $\theta = 90°$, and (*b*) $\theta = 30°$. ——, $M = 0.84$; – – – – – –, $M = 0.78$; — · — · —, $M = 0.68$; — — — —, $M = 0.57$; — · · — · · —, $M = 0.52$; · · · · · · · · · · · ·, $M = 0.59$. $D = 1.27$ cm for $M = 0.59$ case, all others for $D = 2.54$ cm jet.

proportional to L_e. (Thus, $(u'_{fe}/U_e)^2 \approx L_e$ since each curve is for constant M.) This proportionality breaks down at high amplitudes of excitation; and also at high f_p above the cut-on frequency based on the jet diameter. The intercept C in the relationship $20\log(u'_{fe}) = L_e + C$ appeared to be a function of the Helmholtz number $H_D (= St_D M)$. Note that a known functional form for C would have uniquely related u'_{fe}/U_e and L_e. However, a plot of C versus H_D from the resonance data of figure 3 did not yield a continuous function; the spikiness of the resonance characteristics showed up. This matter was also considered beyond the scope of the present study. However, figure 4 clearly indicates the suitability and equivalence of either of u'_{fe}/U_e or L_e for monitoring the excitation level, especially for comparative studies at constant M. For easy cross-reference to the large-scale structure studies u'_{fe}/U_e was chosen as the primary monitoring parameter, the value of L_e corresponding to each case being indicated. This choice was also prompted by the fact that accurate measurement of L_e was more difficult (see e.g. Siddon 1969) and involved the use of a bulkier probe. Furthermore, L_e being strongly dependent on the nozzle reflection coefficient, may be sensitive to the details of the nozzle, which may not be the case for u'_{fe}.

'Plane wave excitation' has been used throughout this study, i.e. all f_p used are below the cut-on frequency based on the jet diameter. Hot-wire traverses across the jet exit, for typical excitation cases, showed that the amplitude distribution

(u'_{fe}/U_e) was uniform over the entire core, and also axisymmetric; but the amplitude increased sharply in the boundary layer. For the excitation case of $St_D = 0.68$ at $M = 0.44$ with an amplitude (u'_{fe}/U_e) of 0.15% in the core, u'_f/U_e increased to about 11% in the boundary layer. Note that variations in the amplitudes and the phase fronts in the boundary layer are typical even at much lower f_p and M (ZH 1980).

The non-dimensionalized power spectral density (PSD) of the far-field noise for the unexcited jet is shown in figure 5 for $0.5 < M < 0.9$. Figure 5(*a*) shows the data for $\theta = 90°$, while (*b*) shows data for $\theta = 30°$. Here,

$$p^* = \left(\frac{p}{\rho U_e^2}\right)^2 \left(\frac{R}{D}\right)^2 \frac{U_e}{D\Delta f},$$

p being the r.m.s. sound pressure in the frequency bandwidth Δf. Based on these, as well as a large set of data from the literature, it was shown that the coordinates used in figures 5(*a*, *b*) best scaled the noise PSD at 90° and 30°, respectively (Zaman & Yu 1985). For the abscissae, the Strouhal number $St_D = fD/U_e$ best collapsed the data for all θ, except at shallow angles where this was achieved with Helmholtz number $(H_D = fD/a_0)$ times the Doppler factor, $(1 - 0.5M\cos\theta)$. The best collapse with the ordinates of figure 5 implied a $U^{6.5}$ and a $U^{8.5}$ scaling for the PSD, and thus a $U^{7.5}$ and a $U^{9.5}$ scaling for the intensity L, at $\theta = 90°$ and 30° respectively; the overall radiated power was found to vary as U^8. (See the above reference for further details.) At low M, the PSD variation became progressively different in shape and amplitude from the curves in figure 5. This deviation was due not only to 'internal noise' but, as will be shown in the following, also to interaction and evolution of the initially laminar shear-layer vortices.

3. Broadband noise suppression

A typical case of broadband noise and turbulence suppression is shown in figure 6 for a Mach number $M = 0.12$ and for excitation at $St_\theta = (f_p\Theta/U_e) = 0.017$. Figure 6(*a*) shows the normalized PSD at $\theta = 90°$ with and without the excitation. The corresponding effect on the longitudinal velocity spectrum (S_u), measured at $x/D = 1.5$ on the jet centerline, is shown in figure 6(*b*). ($\Theta/D = 0.0037$ provides the conversion factor between St_D and St_θ in figures 6–8. The vertical scale for S_u is arbitrary.) Even though the spectral spikes at the excitation frequency (f_p) and its subharmonics in figure 6(*b*) are large, the remarkable suppression of the broadband components of S_u results in a suppression of the total intensity, in this case to 24% of the unexcited level. The corresponding effect on the broadband noise PSD is also remarkable; there is suppression by as much as 10 dB in the middle frequency range, but the large-amplitude tone results in a total intensity which is, in this case, about 13 dB higher than the corresponding unexcited level. (The amplitude variation for the PSD has been checked to be within the dynamic range of the instrumentation.) It was determined, by on-line display of excited versus unexcited noise spectra, for varying U_e and f_p, that maximum broadband noise suppression always occurred at approximately $St_\theta = 0.017$. This same result has also been obtained by Hussain & Hasan (1983). Excitation at this St_θ also induces maximum turbulence suppression, which has been shown by ZH (1981).

Search with the present jet did not yield a total far-field noise suppression. While the total turbulence could be suppressed, the failure to suppress the total sound intensity was disappointing from a practical point of view. As will become clear, even if a total suppression by a few dB were achievable, it is still not promising,

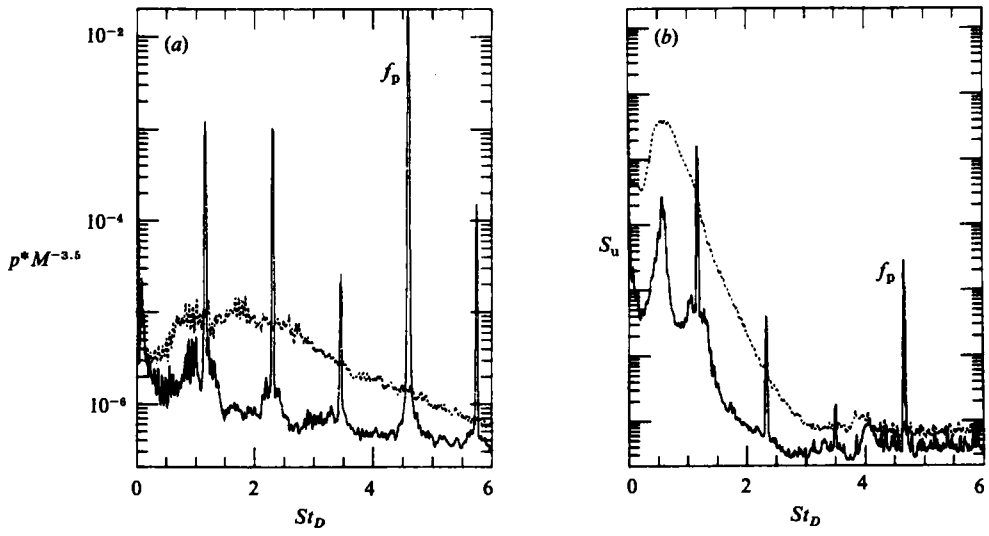

FIGURE 6. Excitation inducing turbulence and broadband noise suppression. Dashed curves for unexcited case. $St_\theta = 0.017$, $u'_{te}/U_e = 0.03\%$, $M = 0.12$, $Re_D = 60000$. (*a*) Noise PSD at $\theta = 90°$, (*b*) u-spectra at $x/D = 1.5$ on jet axis.

because the suppression could only be achieved for jets with initially laminar boundary layers, for which the unexcited noise is already at a higher relative level. (A total noise suppression, by about 1.5 dB, has been reported by Hussain & Hasan (1983). It is not clear why such observation could not be made with the present jet.) However, the dramatic broadband noise suppression (figure 6*a*) is interesting and aeroacoustically intriguing, and merits a full-scale investigation. The principal inferences drawn regarding this phenomenon are enumerated below.

3.1. *St_θ dependence of suppression, and role of vortex pairing*

The noise suppression is found to be dependent upon the Strouhal number of excitation. Significant suppression of the far-field noise occurs in the 'shear-layer mode' of excitation, i.e. at Strouhal numbers falling close to the most unstable mode of the initial shear layer. As discussed above, the optimum occurred at $St_\theta \approx 0.017$.

For excitation at $St_\theta \approx 0.017$, the laminar shear-layer vortices typically go through one or more pairing stages (depending on the ratio D/Θ), within the distance $x/D \lesssim 1$, before the periodicity is gradually lost. Apparently, these pairing stages emit sound as 'tones', yielding the subharmonic spikes in the far-field noise PSD (figure 6*a*; see also Kibens 1980; Laufer & Yen 1983).† Kibens conjectured that the broadband noise suppression is a result of localization of the pairing stages. Excitation removes the jitter from the naturally occurring pairing stages; thus energy is concentrated in

† Hot-wire signals from the jet exit as well as microphone signals from inside the settling chamber showed the existence of these subharmonics in the corresponding spectra. These subharmonics disappeared when St_θ was varied sufficiently to preclude pairing of the vortices. But it was noted that the third stage of pairing which is not 'stable', as inferred from a broad peak in S_u (figure 6*b*), appeared neither in the far-field noise (figure 6*a*) nor in the above signals. Whether the subharmonics in the above signals originated from some peculiarity of the excitation mechanism and triggered the pairing stages, or whether these were the result of an upstream feedback could not be resolved conclusively.

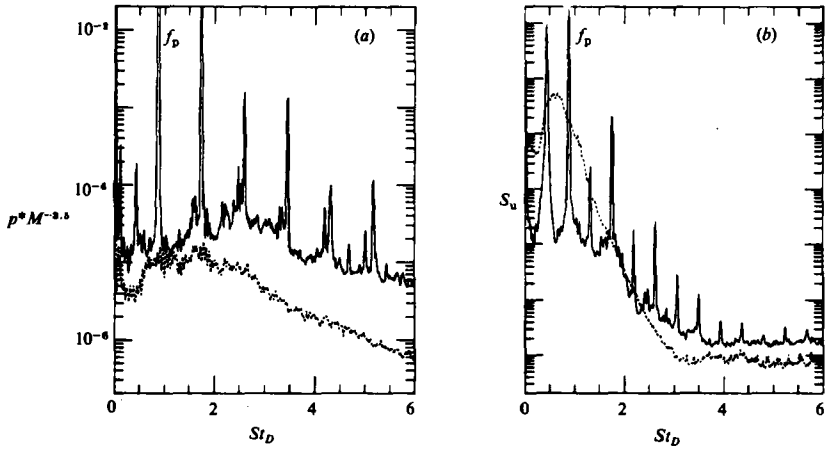

FIGURE 7. Excitation inducing stable vortex pairing. Dashed curves for unexcited case. $St_D = 0.85$, $u'_{te}/U_e = 1\%$, $M = 0.12$, $Re_D = 60000$. (*a*) Noise PSD at $\theta = 90°$, peak amplitude at f_p is 2.0×10^1; (*b*) u-spectra at $x/D = 1.5$ on jet axis.

the subharmonics at the expense of the broadband components. This interpretation appears quite logical; but while it may partially account for the observed suppression it is not a complete account because a localized pairing induced by the excitation does not necessarily result in broadband noise suppression.

Data similar to those in figure 6 are shown in figure 7 for excitation at $St_D = 0.85$, inducing 'jet column mode' pairing. Such pairing was studied extensively by ZH (1980) and HZ (1980): it is characteristic of axisymmetric jets and is different from 'shear-layer mode' pairing in that the lengthscale involved is the jet diameter (D) while it is Θ in the latter case. Excitation at $St_D \approx 0.85$, irrespective of the initial boundary-layer state, results in strong pairing activity within the range $1.5 \lesssim x/D \lesssim 4$, the location being farther upstream within this range for higher St_D and higher excitation level. For an initially laminar boundary-layer case, irrespective of the thickness Θ, this excitation induces a 'stable', i.e. periodic, pairing phenomenon. (But for an initially turbulent or transitional boundary-layer case, the pairing event becomes somewhat, but not completely, random so that an unambiguous subharmonic peak is always detectable in S_u when measured near the pairing location.) Figure 7 represents a case of stable jet column mode pairing. For the same unexcited flow as in figure 6, this localized pairing results in a large broadband noise amplification, as can be seen in figure 7(*a*). (Note that the tone amplitude at the excitation frequency has been indicated in the figure caption, for all PSD data, if it exceeded the ordinate range.)

Observe that a clear but small subharmonic peak is visible in figure 7(*a*). As we shall see later, when the induced jet column mode pairing is not periodic the subharmonic peak is lost in the radiated noise spectrum. But in any case, the excitation-induced structures and their pairings, periodic or not, are much more localized than the naturally occurring events in the unexcited flow. As a matter of fact, it is reasonable to expect that the effect of excitation, for example in the experiments of Bechert & Pfizenmaier (1975) and Moore (1977), was to organize and localize the coherent-structure evolution. Yet the effect of such localization in all these experiments has been an amplification of the broadband noise. This is where Kibens' hypothesis faces a conflict, even though he noted that the increased jitter in the jet column mode excitation could explain the difference. The mechanism of the suppression

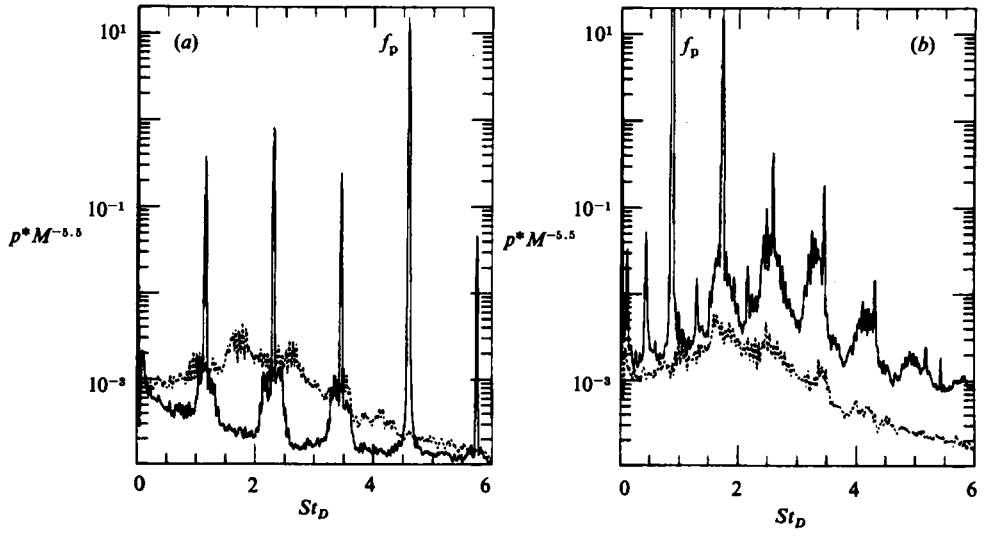

FIGURE 8. Far-field noise PSD at $\theta = 30°$; (*a*) suppression case of figure 6, (*b*) vortex-pairing case of figure 7, peak amplitude at f_p is 1.7×10^3.

phenomenon is closely linked to an initial-condition effect on the coherent structure as well as on the radiated noise, which is discussed in the following subsections.

Here, let us further compare, based on previous experimental results (ZH 1980, 1981; HZ 1980), the two types of pairings involved in figures 6 and 7. In the shear-layer mode, laminar vortices pair to yield laminar vortices, at least in the first one or two stages. In comparison, the (stable) jet column mode pairing occurs farther downstream and is known to be a violent event followed by transition. Thus, the jet column mode pairing is expected to yield a train of pressure pulses whereas a smoother variation of the sound pressure is expected in the other case. (There is experimental evidence that vortex pairing yields large sound-pressure variation; e.g. Sarohia & Massier (1977), HZ (1980). Numerical studies also show large pressure variation associated with vortex pairing; J. C. Hardin, private communication.) One would thus expect stronger subharmonic tones in the shear-layer mode pairing (figure 6) but relatively more spectral broadening in the jet column mode pairing (figure 7). This could partly explain the relatively small subharmonic spike in figure 7 (*a*), which will be further discussed in §4.3.

The observed broadband noise suppression (figure 6*a*) and amplification (figure 7*a*) are essentially independent of the angle of observation, as shown by corresponding normalized PSD for $\theta = 30°$ in figure 8.

3.2. *Effect of exit boundary-layer state*

One of the most significant results of this investigation was that the suppression, as profound as in figure 6(*a*), could not be observed under any excitation condition for an initially tripped jet or for an untripped jet operated at high M. This was a phenomenon observable only in jets with laminar exit boundary layers. The boundary-layer characteristics in the present jet (figure 2) thus permitted the suppression phenomenon to be observed only for $Re_D \lesssim 10^5$.

Based on data from the literature, Crighton (1981) has observed that artificial excitation results in an amplification of the broadband spectral components of turbulence and/or far-field noise if the jet Reynolds number is above 10^5, but a

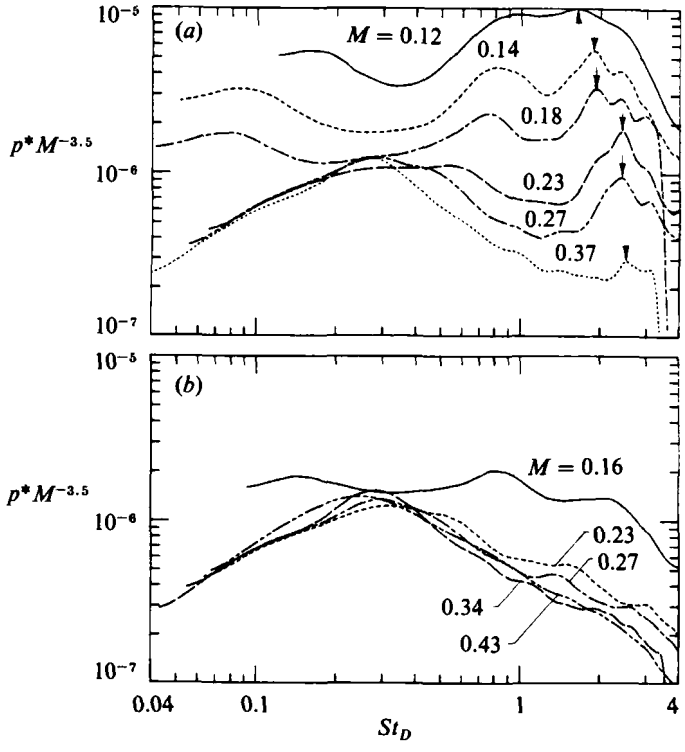

FIGURE 9. Far-field noise PSD at $\theta = 90°$ for low Mach numbers. (*a*) Untripped jet, (*b*) tripped boundary-layer case.

suppression occurs for lower Re_D. The present results strongly suggest that this observed dependence on Re_D enters indirectly, through a dependence on the initial boundary-layer state. (This inference would imply that the transitional Re_D was the same ($\approx 10^5$) in all the experiments summarized by Crighton as well as in the present experiment. This appears to be a coincidence; but it may not be surprising since these experiments involved laboratory model jets with comparable designs and dimensions.)

3.3. *Suppression mechanism and jet noise at low M*

Let us go back to the noise PSD at $\theta = 90°$ in figure 6(*a*) and examine the trace for the unexcited jet. Comparison with figure 5(*a*) reveals that the normalized PSD level at the low M is much higher than the 'asymptotic' level at higher M. The deviation of the noise intensity at low M, from a 'well behaved' U^8-law, is well known and has been generally attributed to 'internal noise' and other 'parasitic' noise sources. It appears from figure 6(*a*) that the optimum suppression at $St_\theta = 0.017$ can only reduce this already high PSD level at most to the asymptotically lower level.

The unexcited jet noise PSD are shown in figure 9(*a*) for different low Mach numbers. One observes a progressive increase of the normalized amplitude with decreasing M. The curves for low M are also characterized by certain high-frequency peaks. (The exact shape and amplitude of the PSD data, especially at low M, were very sensitive to small changes in jet internal configuration; every time the nozzle was remounted, some differences occurred. However, a few sets of data retained the gross features, viz an increasing normalized amplitude with decreasing M and the appearance of the high-frequency peaks.) It was found that a U^3-scaling for the PSD,

and therefore a U^4-scaling for the intensity L, was appropriate for the data of figure 9(*a*). A U^4-scaling for L traces to a monopole source (see e.g. Ribner 1964); thus, such scaling leads one to speculate that the origin of the low-M noise is internal to the jet facility, because the internal noise acts like a monopole at the nozzle exit. However, the observed suppression phenomenon suggests that at least part of this noise must be downstream in origin, because the plausible and most likely mechanism of the suppression is via a change in the downstream coherent-structure dynamics. Indeed, that a significant contribution to the low-M jet noise comes from the interaction of the shear-layer vortices becomes clear by an inspection of the high-frequency peaks in figure 9(*a*).

The dominant high-frequency peak in each curve is marked by an arrow. If one computes the Strouhal number St_θ corresponding to these peaks, this is found to lie in a narrow range: $0.0055 < St_\theta < 0.0065$. Similar peaks in low-$M$ jet noise spectra have also been observed by Bridges and Hussain at the University of Houston (private communication). This St_θ corresponds to half of the initial roll-up frequency for the shear-layer vortices. (The roll-up frequency has been found in different experiments, including others, to correspond to $St_\theta \approx 0.012$, which is considerably lower than the 'most unstable' St_θ of 0.017. The reason for this is not clear, but note that the thickness θ is measured at the exit while the corresponding θ at the roll-up location is higher; this may partly account for the lower St_θ corresponding to the roll-up frequency. See further discussion in ZH (1981).)

Thus, the first stage of pairing of the laminar shear-layer vortices should be emitting sound to cause the high-frequency peaks in the noise PSD. This inference is confirmed by the fact that these peaks are eliminated, and also the PSD amplitude is considerably reduced, when the jet is tripped to eliminate the laminar vortices. This behaviour is demonstrated in figure 9(*b*). For $M \lesssim 0.16$, the data showed a return to trends as in figure 9(*a*), most likely due to relaminarization of the boundary layer. Thus, the dominant noise-production mechanism for low-M jets with initially fully laminar boundary layers must be different from that for high subsonic jets. Not only does additional noise from the interaction of the shear-layer vortices appear, but the background 'jet noise' level is also higher. This is believed to be due to stronger 'laminar-like' structures evolving and dominating downstream in this flow (ZH 1981). The suppression phenomenon under excitation at $St_\theta = 0.017$ is due to a reduction of this additional noise through quick 'saturation' and transition of the laminar vortices, resulting in weaker coherent structures downstream. This transformation in the coherent-structure dynamics also formed the basis for the explanation of the corresponding turbulence suppression provided in ZH (1981). The description of the 'laminar-like' structures, and their dynamics with and without excitation, is supported by flow-visualization pictures and conditionally sampled vorticity data reported in the above reference.

As stated earlier, it was observed that excitation at $St_\theta \approx 0.017$ can, at the most, bring down the broadband PSD to the asymptotically lower level. In this respect, the suppression phenomenon is equivalent to simply tripping the jet boundary layer. The behaviour of the near flow-field turbulence is worth noting in this connection. Figure 10 shows the centerline distribution of u' for a case of suppression ($St_\theta = 0.017$) together with the corresponding unexcited case, a tripped boundary-layer case, and a high-M case. Corresponding variation for a typical 'jet column mode' pairing ($St_D = 0.80$) is also included. Over the distance $0 \lesssim x/D \lesssim 8$, the amplitude for the unexcited low-M case is much higher, and excitation at $St_\theta = 0.017$ brings this down (indicated by the arrow) to a level comparable to the lower levels observed for the

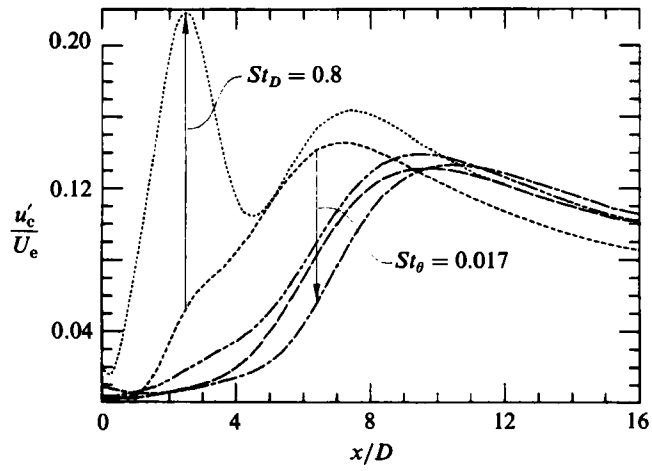

FIGURE 10. Variation of longitudinal turbulence intensity on the jet axis. – – – – – – – –, unexcited 2.54 cm jet at $M \approx 0.03$ (ZH 1981); — · — · —, above jet excited at $St_\theta = 0.017$ (ZH 1981); – – – – – – – – – – – –, above jet excited at $St_D = 0.80$ (ZH 1980); — – – — – – —, unexcited 5.08 cm (tripped) jet at $M \approx 0.09$ (Crow & Champagne 1971); — — — — —, present data for unexcited 2.54 cm jet at $M = 0.44$.

initially tripped, or the high-M, case. (The $St_\theta = 0.017$ case distribution is the lowest, perhaps indicating the scope of some further suppression for the latter two cases.) However, one observes that large-amplitude u_c' in the near flow-field is associated with additional broadband noise in the far field. This simplistic correspondence is, of course, true for the case of excitation at $St_D = 0.8$, which yields an increase in the broadband noise and is associated with large u_c' due to a violent subharmonic generation. It will be shown in the following that pairing of the jet column mode vortices, 'stable' or not, holds the key to broadband jet noise amplification under excitation.

4. Broadband noise amplification

4.1. *Characteristics of noise amplification and excitation amplitude effects*

Figure 11 shows a typical case of broadband noise amplification, for four different excitation levels, for $M = 0.44$ and $St_D = 0.44$. The excitation levels, in terms of u_{fe}'/U_e and L_e, are given in the figure caption. Throughout the rest of this paper, the broadband noise amplification process is discussed by direct comparison of the PSD, with and without excitation, as in figure 11. No effort has been made to further quantify this amplification because that would involve filtering of the tone and its harmonics, either electronically or digitally, each of which could be subjective. Furthermore, the spectral information for the amplification is retained in this way, which would have been lost otherwise due to averaging.

An estimate of the rate of broadband noise increase (figure 11), in the format of Moore (1977), is found to be 0.25 dB per 1 dB increase in L_e. This rate is comparable to, but somewhat lower than, that found by Moore for corresponding St_D and M. One should exercise caution in attaching too much significance to this difference and also to the quantity under consideration itself. A linear response is implicit in using this rate as an indicator of the optimum noise amplification. But the phenomenon being highly nonlinear, a nonlinear response is expected. Indeed, the data of figure 11 and

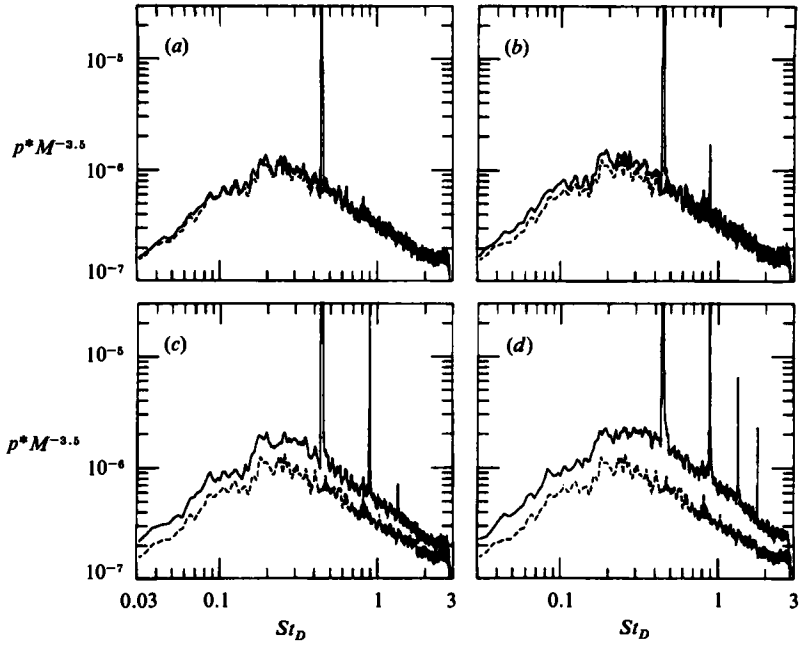

FIGURE 11. Far-field noise PSD at $\theta = 90°$; $M = 0.44$, $St_D = 0.44$. Dashed lines for unexcited jet. u'_{fe}/U_e, L_e and peak amplitude at f_p for the four cases are: (*a*) 0.07 %, 125 dB, 4.1×10^{-4}; (*b*) 0.13 %, 130 dB, 1.4×10^{-3}; (*c*) 0.28 %, 135 dB, 5.9×10^{-3}; (*d*) 0.46 %, 138 dB, 1.6×10^{-2}.

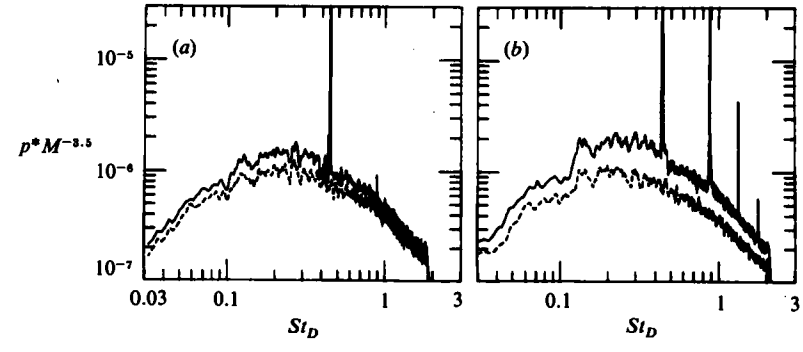

FIGURE 12. Far-field noise PSD at $\theta = 90°$; $M = 0.58$, $St_D = 0.44$. Dashed curves for unexcited jet. u'_{fe}/U_e, L_e and peak amplitude at f_p for the two cases are: (*a*) 0.06 % 130 dB, 1.0×10^{-4}; (*b*) 0.15 %, 136 dB, 6.2×10^{-4}.

another set at $M = 0.58$ (not shown) indicate that the rate of amplification falls off with increasing L_e. One observes, furthermore, that the amount of amplification (and its rate) depends on the unexcited jet noise characteristics. The unexcited jet noise itself is a quantity which is sensitive to small changes in the upstream (i.e. facility internal) configuration. As much as 5 dB scatter was noted among data from the literature representing well-controlled experiments in the field (see Zaman & Yu 1985). Thus, the most viable approach for studying the amplification process seemed to be the simple comparison, on a spectral basis, as in figure 11.

For a given M, keeping u'_{fe}/U_e constant amounts to keeping u'^2_{fe} constant, which reasonably approximates the case of keeping L_e constant (see §2.2). But for a

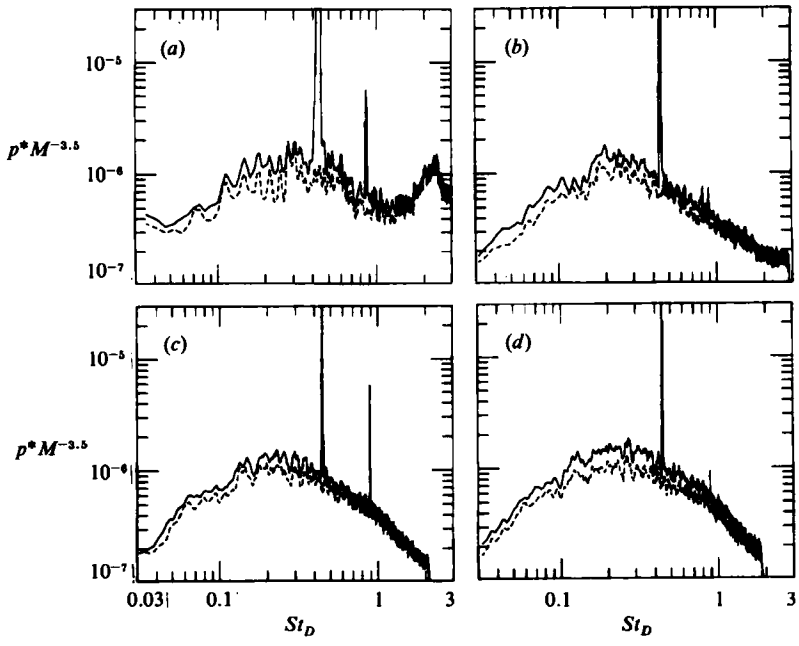

FIGURE 13. Far-field noise PSD at $\theta = 90°$; $St_D = 0.44$, $L_e = 130$ dB. Dashed curves for unexcited jet. M, u'_{fe}/U_e and peak amplitude for the four cases are: (*a*) 0.25, 0.56 %, 2.6×10^{-2}; (*b*) 0.42, 0.13 %, 2.4×10^{-3}; (*c*) 0.58, 0.06 %, 1.1×10^{-4}; (*d*) 0.65, 0.03 %, 1.0×10^{-4}.

constant St_D and for different M, keeping u'_{fe}/U_e constant requires progressively larger u'^2_{fe} and L_e with increasing M. Thus, keeping u'_{fe}/U_e constant is observed to be manifested as an apparent Mach number effect on the broadband jet noise amplification as M is varied; this is demonstrated by the PSD curves of figure 12. Comparison of figures 12(*a*) with 11(*a*), and 12(*b*) with 11(*b*), each pair having approximately the same u'_{fe}/U_e, show that the broadband noise increase is much greater at the higher Mach number. Thus, the 'Mach number effect' inferred from preliminary results of this study and reported by Zaman (1983) could in fact be interpreted as an excitation amplitude effect. For constant L_e, the amplification is found to be approximately the same at different M; this is shown in figure 13. Data for four Mach numbers, all for $L_e = 130$ dB and $St_D = 0.44$, are shown here, and the preceding inference is evident.

4.2. *Effect of excitation level and Mach number on the coherent structure*

Here, let us briefly look into the changes in the large-scale structures occurring under increasing excitation level. Phase-averaged azimuthal vorticity (Ω_z) data are shown in figure 14, obtained by ZH (1984) as well as in the present experiment. The eduction was done at $x/D = 3$ for all four cases. Contours of Ω_z are shown on a cross-sectional plane, as a function of time (τ) and distance (y) from the jet axis. Phase-averaged longitudinal and transverse velocities ($\langle u \rangle$ and $\langle v \rangle$) were first obtained as a function of y and τ; a velocity signal from a fixed single-wire probe at $x/D = 3$ and $y/D = 0.25$ served as the reference signal; the peaks in this signal (larger than twice the standard deviation) represented $\tau = 0$. Ω_z was then obtained via Taylor's hypothesis, using the equation, $\Omega_z = -\partial\langle u \rangle/\partial y - (1/(0.5U_e))\,\partial\langle v \rangle/\partial\tau$. In all four cases, Ω_z has been non-dimensionalized by f_m, and τ by T_m, such that $f_m D/U_e = 0.45$ and $T_m = 1/f_m$.

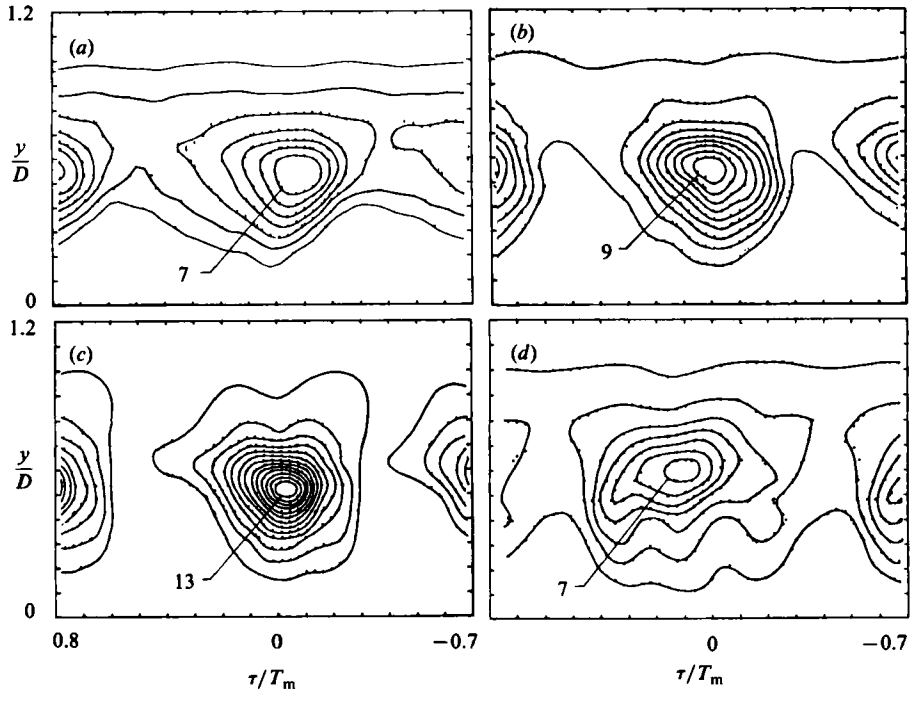

FIGURE 14. Phase-averaged azimuthal vorticity (Ω_z/f_m) measured at $x/D = 3$. Cases (*a–c*) are taken from Zaman & Hussain (1984); $D = 7.6$ cm tripped jet, $M = 0.06$, $Re_D = 110000$, $St_D = 0.49$. u'_{fe}/U_e: (*a*) 0.1%, (*b*) 0.5%, (*c*) 1.5%. (*d*) Data obtained in present experiment; $M = 0.44$, $Re_D = 250000$, $St_D = 0.44$, $u'_{fe}/U_e = 0.15\%$.

For further details, including justification for using $0.5U_e$ as convection speed in Taylor's hypothesis, see the above reference.

Figures 14(*a–c*) represent a low Mach number case with excitation at $St_D = 0.49$, for amplitudes (u'_{fe}/U_e) of 0.1%, 0.5%, and 1.5%, respectively. Note that with increasing excitation amplitude the structures become strengthened, as marked by the increasing peak vorticity in the core. It was demonstrated by ZH (1984) that the 0.1% amplitude was sufficient to make the structures periodic, but the individual structures for this excitation (figure 14*a*) agreed very closely with the natural (unexcited) structure educed by conditional sampling. Measurements in the present jet for $M = 0.44$, $St_D = 0.44$ and $u'_{fe}/U_e = 0.15\%$, for which noise amplification data were shown in figure 11, yielded a roughly similar structure, as shown in figure 14(*d*). The reason for the high-speed side distortions in the contours is not clear, but is believed to be due to varying probe interference in the high Mach number flow as the X-wire probe was drawn out from $y = 0$ while recording the data at different y-stations. Note that the frequency of excitation (f_p) was 2550 Hz in the present case compared to only 144 Hz in figures 14(*a–c*); thus, any jitter in data sampling should cause more smearing in the present case. Note also that the slightly lower St_D in the present case added to a somewhat elongated structure (size and spacing) in figure 14(*d*), because τ was normalized in all cases by T_m.

Despite the distortions, comparison of figures 14(*a*) with 14(*d*) shows that the gross large-scale structure characteristics remain essentially the same at higher Mach numbers. Note that ZH (1984) also demonstrated, for low M, the Re_D independence

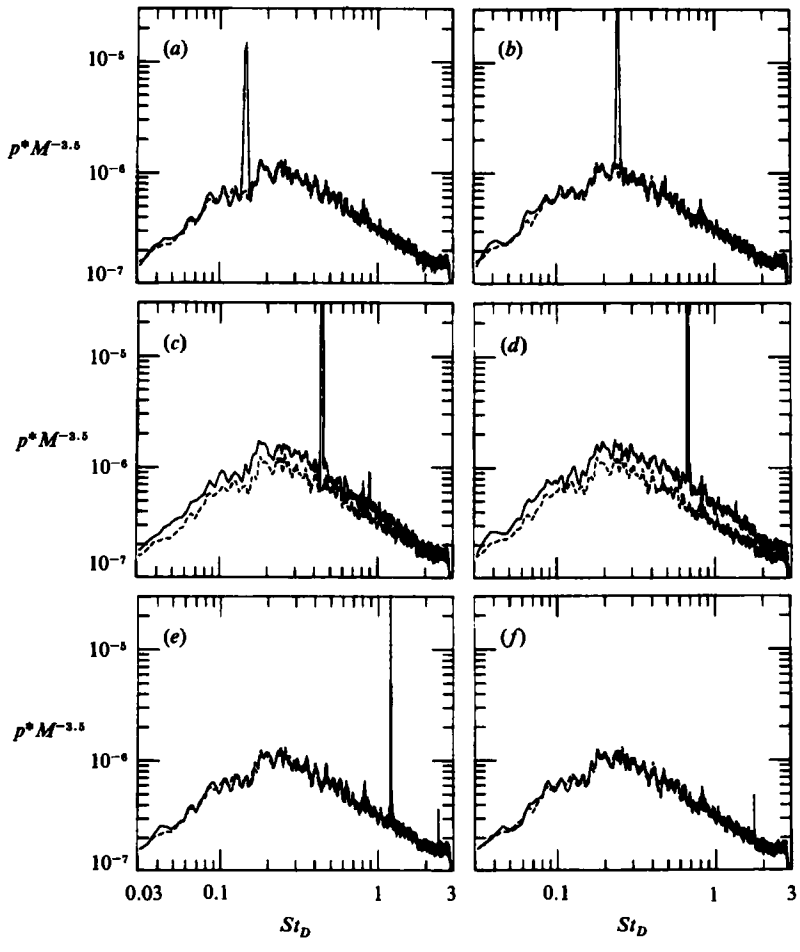

FIGURE 15. Strouhal number effect on far-field noise PSD at $\theta = 90°$; $M = 0.44$, $u'_{te}/U_e = 0.15\%$. Dashed curves are for unexcited cases. St_D, L_e and peak amplitude at f_p for the six cases are: (*a*) 0.15, 121 dB, 1.5×10^{-5}; (*b*) 0.25, 120 dB, 2.2×10^{-4}; (*c*) 0.44, 131 dB, 3.0×10^{-3}; (*d*) 0.68, 134 dB, 1.6×10^{-3}; (*e*) 1.2, 124.5 dB, 2.1×10^{-4}; (*f*) 1.8, 120 dB, 4.9×10^{-7}.

of these structures up to $Re_D \approx 10^6$. Thus, in spite of conjectures to the contrary (Long, Van Lent & Arndt 1980), these data together with such others as the flow-visualization pictures of Moore (1977) should put to rest any lingering doubt about the presence of these structures in jets with high Mach and Reynolds numbers.

4.3. *Strouhal number effect*

Let us now look at the Strouhal number dependence of the broadband noise amplification phenomenon, for which a set of data are shown in figure 15. For $M = 0.44$ and for $u'_{te}/U_e = 0.15\%$ (corresponding L_e indicated), data are shown for six St_D. Inspection of the data shows that $St_D = 0.68$ results in the maximum broadband noise amplification. Corresponding data at $\theta = 30°$, presented in figure 16, also lead to the same inference. Data for the six St_D with L_e constant (130 dB) also showed maximum amplification at $St_D = 0.68$ (these data appeared quite similar to those in figure 15 but are not shown). This result contrasts with the findings in some, and the implicit assumptions in most other, previous studies – that the maximum

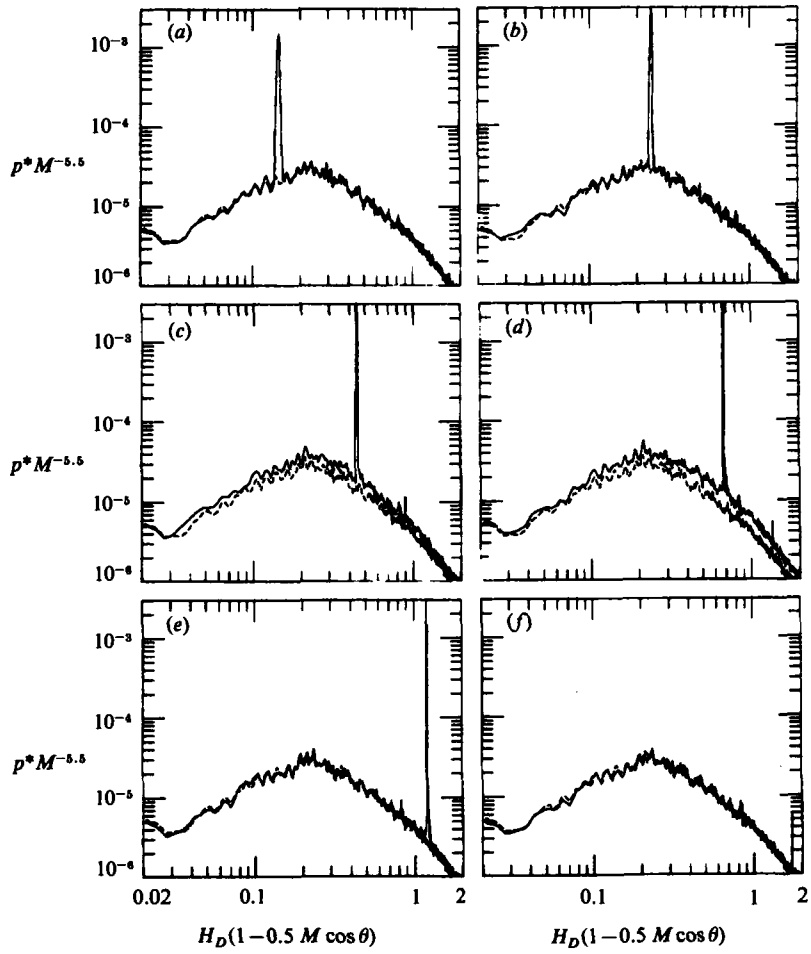

FIGURE 16. Far-field noise PSD at $\theta = 30°$ corresponding to the six cases of figure 15. Peak amplitudes at f_p are: (*a*) 1.7×10^{-3}, (*b*) 5.3×10^{-3}, (*c*) 1.8×10^{-2}, (*d*) 6.6×10^{-2}, (*e*) 5.6×10^{-3}, (*f*) 6.0×10^{-6}.

broadband noise amplification occurs for excitation near the 'preferred mode' Strouhal number; the maximum amplification has been variously observed in the St_D range of 0.35–0.50. However, the data on the St_D effect obtained by Ahuja *et al.* (1982) actually show a closer agreement with the present results; their one-third octave spectral data, obtained with constant L_e show the maximum amplification for excitation St_D of 0.63 rather than at a lower St_D. The results presented by Juvé & Sunyach (1981) also implied that optimum amplification occurred at $St_D = 0.68$ in their experiments.

Two additional pairs of figures (17*a–d*) for two lower Mach numbers are included to show the effect of excitation at $St_D \approx 0.45$ versus that at $St_D \approx 0.75$. For both Mach numbers, $St_D \approx 0.75$ resulted in larger amplification, compared to excitation at $St_D \approx 0.45$. Similar comparison could not be made at higher M, because f_p corresponding to the higher St_D approached the cut-on frequency for helical modes, so that plane wave excitation could no longer be assumed; available excitation amplitudes were also too low at such high f_p. Note that since the resonance frequencies (figure 3) were used for excitation (to obtain large enough amplitudes), St_D could not be

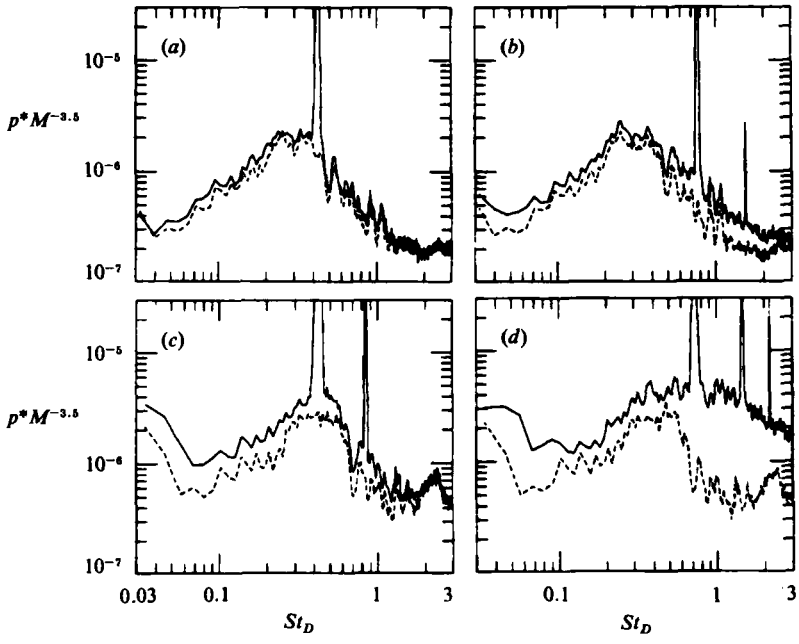

FIGURE 17. Far-field noise PSD at $\theta = 90°$. Dashed curves are for unexcited jet. $M = 0.38$, $u'_{fe}/U_e = 0.27\%$: (*a*) $St_D = 0.42$, (*b*) $St_D = 0.76$. $M = 0.26$, $u'_{fe}/U_e = 1.25\%$: (*c*) $St_D = 0.43$, (*d*) $St_D = 0.73$. Peak amplitudes at f_p for the four cases are: (*a*) 5.4×10^{-4}, (*b*) 9.6×10^{-3}, (*c*) 1.4×10^{-1}, (*d*) 2.9×10^{-2}.

varied continuously. But from these and other data (not shown), it was concluded that the maximum broadband noise amplification occurred in the St_D range of 0.65–0.85.

4.4. *Tone amplitude in the far field*

As mentioned before, the tone amplitude at f_p has been indicated for all PSD data if it exceeded the ordinate range. The question whether the excitation tone gets amplified by the jet column has been addressed in previous investigations (Crow 1972; Moore 1977; Bechert, Michel & Pfizenmaier 1977). By comparison of the radiated tone amplitudes with and without the jet flow on, Crow (1972) inferred that the tone must be amplified by the jet because the amplitude with the flow on was some 30 dB higher. The objection to this inference was that the drastically different transmission characteristics of the nozzle, with and without the flow on, were not taken into account. Subsequently, it was experimentally determined, e.g. in the other two references cited above, that the tone is *not* amplified by the jet column but the power transmitted through the nozzle is merely radiated to the far field. For lower frequencies, there is actually an absorption of the imparted sound.

The amplitudes of the tone at $\theta = 90°$ for the six St_D cases of figure 15 are listed in table 1. These data are for $M = 0.44$ and $u'_{fe}/U_e = 0.15\%$. Also listed in this table are the corresponding tone amplitudes when L_e was held constant. These data show that for either constant u'_{fe}/U_e or constant L_e, the tone intensity is dependent on St_D and maximum at about the preferred mode St_D. Similar data for $\theta = 30°$ also exhibited the same trend. The same trends at 90° and 30° indicate that the integrated radiated power at f_p could also very similarly with St_D. This possibility, together with

St_D	$u'_{te}/U_e = 0.15\%$	$L_e = 130$ dB
0.15	41.9	46.7
0.25	53.5	62.7
0.44	64.9	63.9
0.68	62.1	57.8
1.2	53.3	56.1
1.8	27.1	(L_e not available)

TABLE 1. Sound pressure level (dB) at the excitation tone in the far field ($\theta = 90°$)

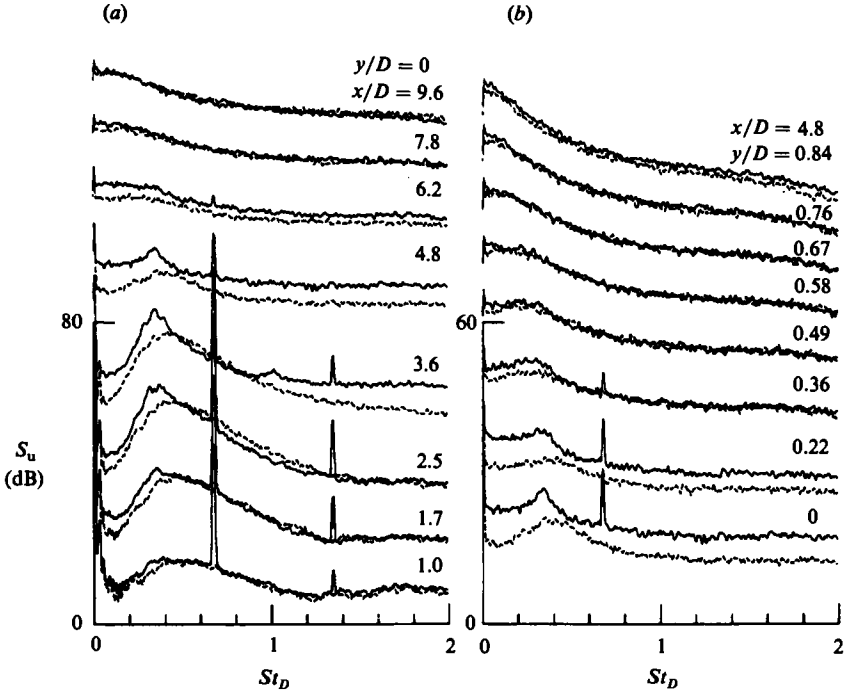

FIGURE 18. Spectra of longitudinal velocity signal (S_u); $M = 0.44$, $St_D = 0.68$, $u'_{te}/U_e = 0.15\%$. Dashed curve are for unexcited case. Ordinate scales are arbitrary. (*a*) S_u for different x on the jet axis, (*b*) S_u for different y at $x/D = 4.8$.

the results stated in the previous paragraph, would imply that the transmitted power through the nozzle also depends similarly on St_D. These appear intriguing but were not pursued any further because of the many difficulties in measurement of the transmitted power.

4.5. *Evidence and role of vortex pairing in noise amplification*

The excitation St_D-range of 0.65–0.85, producing maximum broadband noise amplification, had also been found to induce the 'jet column mode' pairing of the coherent structures (ZH 1980). The pairing activity for the excitation case of figure 15(*d*) is demonstrated in figure 18(*a*) by the longitudinal velocity spectra (S_u) measured at different x on the jet axis. For each x noted in the figure, the corresponding S_u for the unexcited jet is also shown. For the excitation case (solid traces), one observes that a broadband but clear subharmonic peak emerges at $x/D \approx 2.5$; this characterizes

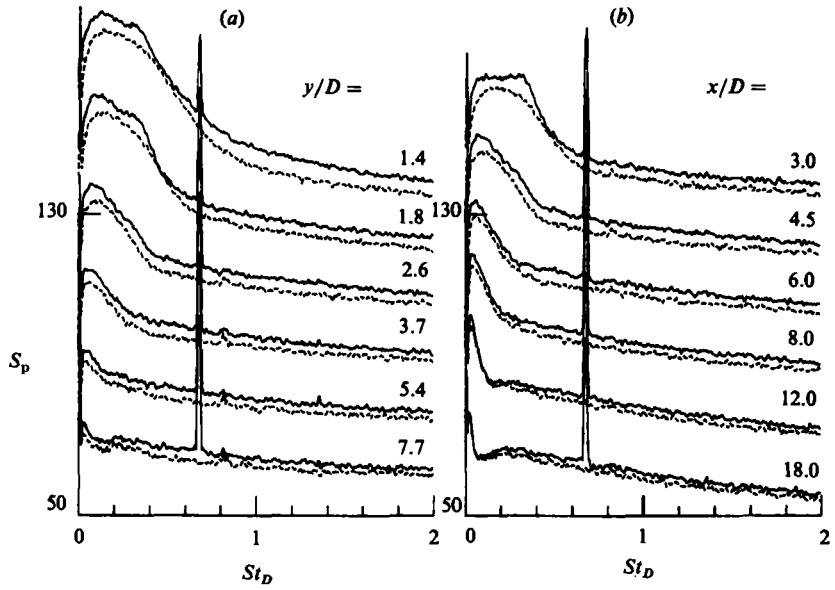

FIGURE 19. Spectra of near sound-pressure field (S_p, dB); $M = 0.44$, $St_D = 0.68$, $u'_{te}/U_e = 0.15\%$. Dashed curves are for unexcited case. (*a*) S_p for different y at $x/D = 4.5$, (*b*) S_p for different x along $\theta \approx 30°$ line.

the spectra through the station $x/D = 4.8$, indicating the pairing activity taking place in this axial range. Note that the only plausible mechanism for the subharmonic generation in the flow under consideration is vortex pairing.

As shown by ZH (1980) and HZ (1980), the subharmonic in S_u emerges as soon as two vortices in alternate pairs begin to be drawn towards each other; the subharmonic grows to a maximum when the faster-moving inner vortex ring catches up and is inside the slower-moving outer one. The pairing process culminates farther downstream with a violent engulfment of the inner vortex by the outer one, a significant spectral broadening taking place in S_u measured at that location. Accordingly, the pairing process completes in the present flow somewhere around $x/D = 4.8$. Note that the sequence of these events occurred farther upstream in the above studies because a much higher excitation amplitude (3%) was employed for a case of 'stable' pairing.

In figure 18(*b*), spectra S_u at different y across the mixing layer are shown for $x/D = 4.8$, as in figure 18(*a*). One finds that the turbulence amplification is at a maximum near the jet axis, is not noticeable inside the mixing layer and is again observable on the low-speed side. The sound pressure spectra (S_p) in the vicinity of the jet are examined in figure 19 for the $St_D = 0.68$ case. Figure 19(*a*) shows S_p for different y at $x/D = 4.5$, while (*b*) shows that for different x but along a $\theta \approx 30°$ line. One observes that the subharmonic peak does not appear clearly in S_p, except near the edge of the jet where only a bulge appears. The subharmonic peak was also not detectable in the corresponding far-field noise PSD (figures 15*d* and 16*d*). Recall that the localized pairing of the laminar vortices in the shear-layer mode of excitation yielded the subharmonic peaks even in the far field (figure 6). A small but clear subharmonic peak was also observed in the noise PSD for the 'stable' jet column mode pairing in figure 7.

Thus, it is apparent that the jitter associated with the present 'unstable' pairing

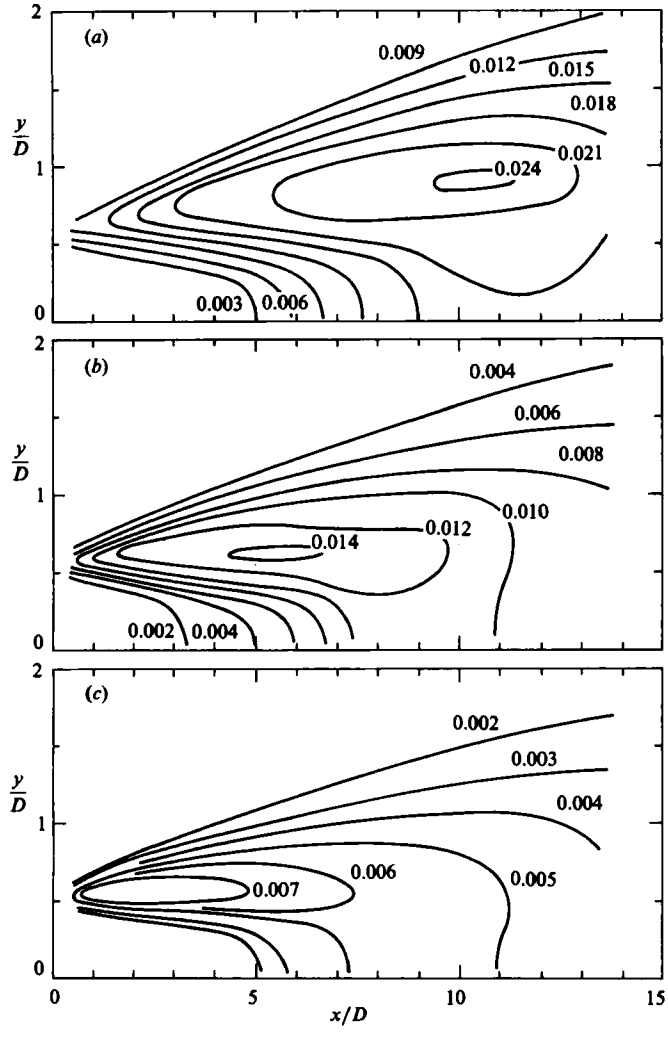

FIGURE 20. Contours of filtered r.m.s. velocity fluctuation, non-dimensionalized by U_e, for the unexcited jet at $M = 0.44$. St_D corresponding to the three spectral components are: (*a*) 0.1, (*b*) 0.34, (*c*) 1.0.

process (at $St_D = 0.68$) is sufficient to smear out the subharmonic peak in S_p. This is not surprising, because while S_u captures the events in the flow at a point, S_p is an integrated effect at the measurement point from a volume of the noise-producing region in the flow. Furthermore, while S_u is due to time variation of the flow events at the measurement point, the origin of the sound radiation should be linked to double derivatives of these flow 'events' (e.g. Lighthill 1952). Thus, jitter in the pairing which broadens the subharmonic peak in S_u ought to appear in magnified proportions in the corresponding radiated sound.

The details of the noise amplification for the $St_D = 0.68$ case, for the flow-field and the near sound-pressure field, are shown in figures 20–22. Data for the unexcited jet at $M = 0.44$ are first shown in figures 20 and 21. The amplitude distributions for three spectral components, *viz* $fD/U_e = 0.1$, 0.34 and 1.0, are presented as contour maps. Note that the 0.34 component corresponds to the subharmonic (for the excitation

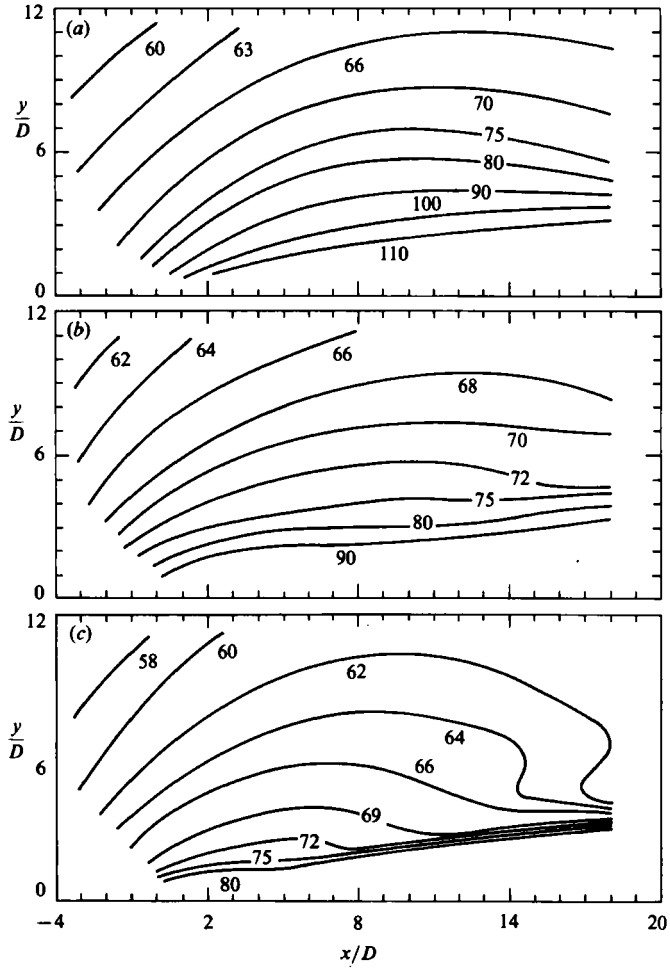

FIGURE 21. Contours of filtered sound pressure level (dB) for the unexcited jet at $M = 0.44$. St_D corresponding to the three spectral components are: (*a*) 0.1, (*b*) 0.34, (*c*) 1.0.

case), while 0.1 and 1.0 are two non-(sub)harmonic components. Figure 20 shows the spatial distribution of each of these three components, corresponding to the S_u data for the flow-field. That is, these are the filtered r.m.s. velocity fluctuations obtained from similar S_u data to those in figure 18, but measured at many spatial grid locations. (Data were obtained for 11 y-stations per x-station, with slowly diverging grids downstream.) One observes that the amplitude of these spectral components generally decreases with increasing frequency, that the peak amplitudes occur in the middle of the mixing layer in all cases, and that the location of the peaks moves upstream with increasing frequency. Corresponding amplitude distributions for the (unexcited) near-field sound pressure outside the jet are documented in figure 21. The details of these spectral characteristics, together with the total turbulence intensities, Reynolds stress, etc., for an unexcited subsonic jet, have been discussed by Zaman (1985). Here, let us concentrate on the changes brought in these distributions by the excitation at $St_D = 0.68$.

Excitation results in a shift of the contours of figures 20 and 21. However, since the amount of amplification is small compared to the basic levels, it is difficult to

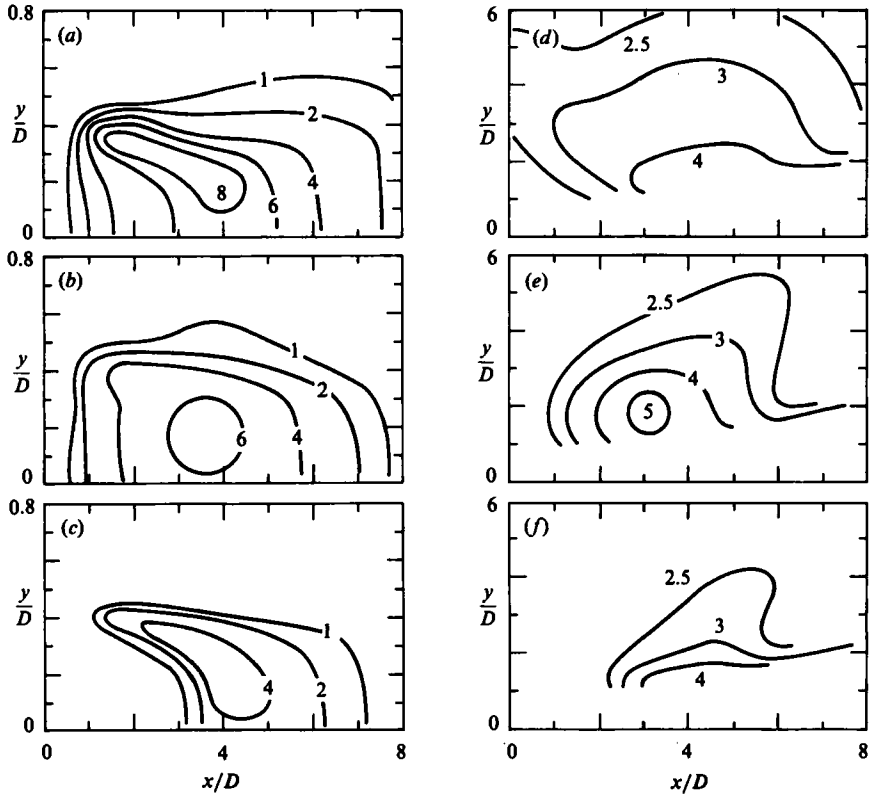

FIGURE 22. Broadband noise amplification (over the unexcited levels of figures 20 and 21, in dB) for excitation at $St_D = 0.68$, $M = 0.44$, $u'_{te}/U_e = 0.15$ percent. (*a*) (*b*), and (*c*) are for flow spectral components of $St_D = 0.1, 0.34$, and 1.0, respectively. (*d*), (*e*), and (*f*) are for near-field sound pressure spectral components of $St_D = 0.1$, 0.34, and 1.0, respectively.

discern the changes in similar contour maps for the excitation case. A clearer perception of this change is obtained from the distribution of the ratio of the excited and the unexcited levels. This amplification (in dB) for each of the three spectral components, for the flow and for the near-field sound, is shown in figure 22: (*a–c*) show the amplification for S_u; (*d–f*) show that for S_p. As observed from the spectral traces of figure 18, figure 22 (*b*) shows clearly that the maximum amplification of the subharmonic occurs in a region nearer to the jet axis and shortly upstream of $x/D \approx 4$. Figures 22 (*a*) and (*c*) show that the maximum broadband turbulence amplification also occurs in this same spatial region. More significantly, one observes that the maximum noise amplification also takes place precisely in this same axial range. It transpires from these data that the pairing activity under the excitation plays the crucial role, like a localized source region, in contributing to the broadband noise amplification.

5. Concluding remarks

The roles of the large-scale coherent structures in broadband jet noise suppression and amplification, under controlled excitation, have been investigated. The suppression occurs only at low Reynolds numbers and Mach numbers when the boundary layer at the jet exit is laminar. For such jets, the broadband noise, as well as the near

flow-field turbulence suppression occurs in the 'shear-layer mode' of excitation, maximum taking place at $St_\theta \approx 0.017$. However, while the total turbulence intensity could be suppressed well below the corresponding unexcited level, suppression of the noise could be observed only for the broadband components.

Kibens (1980) proposed an explanation of the broadband noise suppression, to be due to localization of vortex pairing. Present data demonstrate that only a localization of pairing cannot explain the suppression. The suppression mechanism is also related to the noise-production mechanism in jets with laminar initial boundary layers. The noise PSD of such jets is at a higher relative level compared to that for jets with initially turbulent boundary layers; the initial-condition effect has been demonstrated by tripped versus untripped jet data. Stronger 'laminar-like' coherent structures form and dominate the entire near flow-field of jets with laminar initial condition; thus, as had been shown by ZH (1981), the turbulence intensities, Reynolds stress, etc. exhibit atypically large amplitudes. The evolution and interaction of these stronger coherent structures are believed to cause the higher (normalized) noise level. Part of the contribution to the higher noise level could be traced to the first stage of pairing of the initially laminar vortices. Excitation at $St_\theta \approx 0.017$ results in an early roll-up, pairing and breakdown of the initial vortices, yielding 'weaker' coherent structures downstream. This transformation in the coherent-structure dynamics in the entire near flow-field appears directly to cause the suppression of turbulence as well as of broadband noise. The 'weaker' coherent structures thus formed are similar to the structures in jets with initially turbulent/transitional boundary layers; thus, the turbulence and noise are suppressed at the most to the asymptotic levels which occur for the high-speed jets.

The dependence of the jet response to excitation on initial condition ought to explain Crighton's (1981) observation of the Reynolds number dependence for broadband noise amplification/suppression. The effect of initial boundary-layer state on the unexcited jet noise raises serious questions about the applicability of results from low-M jets having laminar boundary layers to the noise production mechanism of high subsonic jets. Note that the observed effect of the initial boundary-layer state on the unexcited jet noise, to the best of the author's knowledge, is clearly documented for the first time in this study. Present data show that a more consistent U^8-scaling for the radiated noise power is achieved, over a wider speed range, for tripped jets. However, tripping does not necessarily guarantee a transitional (let alone a fully turbulent) boundary layer; there can be relaminarization at low speeds and, thus, a return to deviation from the 8th-power law.

When the unexcited jet noise is at the asymptotically lower level, excitation can only result in an amplification of the broadband noise. The crucial link between the noise-amplification mechanism and the coherent-structure dynamics emerged from the Strouhal number dependence of the phenomenon. It is demonstrated in this study that maximum broadband noise amplification occurs in the St_D range where strongest vortex-pairing activity is induced. Moore (1978) had also observed, via telescopic source location, that the broadband noise from the jet appeared to come from 'the position where the vortices interact in the Schlieren photographs...'. The pairing activity, corresponding to excitation producing significant broadband noise amplification, was also recognized by Juvé & Sunyach (1981). In the present work, it has been shown through detailed spectral measurements of the flow and the near-field sound that the noise amplification originates from around the pairing location.

5.1. *Further remarks*

The pairing process under consideration involves some jitter; thus, the velocity spectrum measured near the pairing location is characterized by a hump, instead of a sharp peak, at the subharmonic frequency. In the spectrum of the radiated sound, however, the subharmonic hump is not observable. This raises a question in regard to the present conclusion that pairing is responsible for the noise amplification. One might argue that, if pairing were responsible, the subharmonic peak should have appeared in the noise spectrum. However, the absence of the subharmonic could be reconciled as follows. First, the far-field (as well as near-field) noise measured at a point is an integrated effect of the contribution from the entire flow-field; thus, jitters from different parts of the flow, axial and azimuthal, have a cumulative broadening effect. Secondly, while the velocity spectrum captures the flow events at the measurement point in the flow, the origin of the sound radiation is linked to spatial (or temporal) derivatives of the 'flow events'; thus, jitters in the flow are expected to appear in magnified proportions in the noise. It seems that this ought to explain why one observes only the broadband amplification even though the origin of this amplification is in the induced pairing activity.

Note that the pairing process considered in the present study is of the axisymmetric coherent structures. Broadband noise amplification has also been observed under azimuthal mode excitation (Bechert & Pfizenmaier 1977; Ahuja *et al.* 1982), which ought to involve helical coherent structures. One could speculate that some combination of tearing and pairing of these structures, induced by the excitation, may also be the primary cause for the corresponding broadband noise amplification.

It is to be emphasized that the present results, both on suppression and amplification, point towards a direct role of the large-scale structures in the noise modification. For the suppression, a direct role is evident; the phenomenon could be reconciled in terms of the change in the large-scale structure dynamics; the noise radiation at the subharmonics also bears witness to this. A direct radiation, for low-M jets with initially laminar boundary layers, has been the conclusion of Laufer & Yen (1983). (However, they apparently did not recognize the profound initial-condition effect on jet noise.)

A passive and indirect role of the large-scale structures in the noise radiation was first suggested by Moore (1977) based on the results of the 'tone amplification' experiments, which have been described in the text. Since then, a direct versus indirect role of the large-scale structures in jet noise production has been a point of contention. A direct role can be thought of as radiation from a certain phase of evolution (roll-up–growth–saturation) of the structures ('instability waves'), or from the interaction (like pairing) of the structures. An indirect role, on the other hand, has been thought of as radiation, primarily from small-scale structures which in turn are modified by the large-scale structures. In some respects, however, the division in the two schools of thought is a thin line. Proponents of an indirect role (e.g. Ribner 1981) accept the view that the large-scale structures strongly influence the flow dynamics. (Ribner, in this reference, attempts to integrate the roles of small- and large-scale structures in noise radiation.) From the controlled excitation studies, it is known that small-scale turbulence is organized by the large-scale structures. Consider, for example, the 'quadrupole' type distribution of the 'incoherent' Reynolds stress (due to small scales) around a large-scale structure (HZ 1980). If the noise radiation is caused by the advection of such a stress distribution riding on the large-scale structure, then the question of direct versus indirect role can merely be a matter of semantics.

However, in connection with the broadband noise amplification, some of the evidence put forward in support of an indirect role is questionable. For example, one can question the definitions of 'large-scale turbulence' and 'small-scale turbulence' used by Ahuja *et al.* (1982) (showing that only the latter is affected by forward flight and thus suggesting an indirect role of the former in the noise amplification). In flows where the 'large-structure turbulence' would be zero according to this definition, the dominance of the large structures has been demonstrated by many (see e.g. HZ 1984). The spectral uniformity of the broadband noise amplification has been cited to favour an indirect role, the logic being that the amplification should have occurred over a narrow frequency band around the excitation frequency if the large structures radiated directly. This can be countered by the same arguments as stated in this section on why the subharmonic peak does not appear in the radiated noise spectra. Note that Moore's inference, which initially brought up the above question, has been criticized by Laufer & Yen (1983) as being 'hastily drawn'. It has also been seriously questioned by Michalke (1983). Even though vortex pairing was not taken into consideration, Michalke's analysis showed noise radiation, at low H_D, primarily occurring from large-scale rather than small-scale structures. It is furthermore apparent that, while conclusions had been drawn about the indirect role of the large-scale structure, the role of vortex pairing had not been fully recognized. Maximum broadband noise amplification was assumed to occur for excitation at the 'preferred mode' St_D, while it is shown here that this occurs for a higher St_D range where pairing is induced.

Finally, it should be recognized that the present results suggest but are not conclusive about a direct role of the large-scale structures in the natural (unexcited) jet noise production. Further study will be required to determine how direct this role is: whether pairing or a stage of evolution of the structures contribute most to the unexcited jet noise PSD that is remarkably characterized by a peak near the 'preferred mode' Strouhal number.

This research was carried out while the author held a National Research Council Associateship. The author is grateful to the NRC-NASA Associateship Program for the support, to Dr J. C. Yu for many valuable discussions during the course of this study and for reviewing the manuscript, and to Professor H. S. Ribner for making detailed critical comments on the material presented in the paper.

REFERENCES

Ahuja, K. K., Lepicovsky, J., Tam, C. K. W., Morris, P. J. & Burrin, R. H. (Lockheed-Georgia Co.) 1982 Tone-excited jet–theory and experiments. *NASA-CR-3538.*

Browand, F. K. & Laufer, J. 1975 The role of large-scale structures in the initial development of circular jets. *Turb. in Liquids* **5**, 333.

Bechert, D. W. & Pfizenmaier, E. 1975 On the amplification of broadband jet noise by a pure tone excitation. *J. Sound Vib.* **43**, 581–587.

Bechert, D. W. & Pfizenmaier, E. 1977 Amplification of jet noise by a higher-mode acoustical excitation. *AIAA J.* **15**, 1268–1271.

Bechert, D. W., Michel, U. & Pfizenmaier, E. 1977 Experiments on the transmission of sound through jets. *AIAA Paper*-77-1278.

Chan, Y. Y. 1974 Spatial waves in turbulent jets. *Phys. Fluids* **17**, 46–53.

Crighton, D. G. 1981 Acoustics as a branch of fluid mechanics. *J. Fluid Mech.* **106**, 261–298.

Crow, S. C. 1972 The predictability of jet noise. *NASA Lecture on 10 January* RFP-6-8442-SC-158.

CROW, S. C. & CHAMPAGNE, F. H. 1971 Orderly structures in jet turbulence. *J. Fluid Mech.* **48**, 547–591.

DENEUVILLE, P. & JACQUES, J. R. 1977 Jet noise amplification: a practically important problem. *AIAA Paper*-77-1368.

FFOWCS WILLIAMS, J. E. & KEMPTON, A. J. 1978 The noise from the large-scale structure of a jet. *J. Fluid Mech.* **84**, 673–694.

HO, C.-M. & HUANG, L.-S. 1982 Subharmonics and vortex merging in mixing layers. *J. Fluid Mech.* **119**, 443–473.

HUSSAIN, A. K. M. F. 1980 Coherent structures and studies of perturbed and unperturbed jets. *Lecture Notes in Physics* vol. **136** (ed. J. Jiminez), 252–291.

HUSSAIN, A. K. M. F. 1983 Coherent structures and incoherent turbulence. Paper at *IUTAM Symposium on Turbulence and Chaotic Phenomena in Fluids, Kyoto.*

HUSSAIN, A. K. M. F. & HASAN, M. A. Z. 1984 Turbulence suppression in free turbulent shear flows under controlled excitation. Part 2. Jet noise suppression. (Submitted to *J. Fluid Mech.*)

HUSSAIN, A. K. M. F. & ZAMAN, K. B. M. Q. 1980 Vortex pairing in a circular jet under controlled excitation, Part 2. Coherent structure dynamics. *J. Fluid Mech.* **101**, 493–544.

HUSSAIN, A. K. M. F. & ZAMAN, K. B. M. Q. 1981 The 'preferred mode' of an axisymmetric jet. *J. Fluid Mech.* **110**, 39–71.

JUBELIN, B. 1980 New experimental studies on jet noise amplification. *AIAA Paper*-80-0961.

JUVÉ, D. & SUNYACH, M. 1981 Near and far field azimuthal correlations for excited jets. *AIAA Paper*-81-2011.

KIBENS, V. 1980 Discrete noise spectrum generated by an acoustically excited jet. *AIAA J.* **18**, 434–441.

LAU, J. C., FISHER, M. J. & FUCHS, H. V. 1972 The intrinsic structure of turbulent jets. *J. Sound Vib.* **22**, 379–406.

LAUFER, J. & YEN, T.-C. 1983 Noise generation by a low-Mach-number jet. *J. Fluid Mech.* **134**, 1–31.

LIGHTHILL, M. J. 1952 On sound generated aerodynamically: I. general theory. *Proc. R. Soc. Lond.* **A211**, 564–587.

LONG, D., VANLENT, T. & ARNDT, R. E. A. 1981 Jet noise at low Reynolds numbers. *AIAA Paper*-81-1962.

MICHALKE, A. 1983 Some remarks on source coherence affecting jet noise. *J. Sound Vib.* **87**, 1–17.

MOORE, C. J. 1977 The role of shear-layer instability waves in jet exhaust noise, *J. Fluid Mech.* **80**, 321–367.

MOORE, C. J. 1978 The effect of shear layer instability on jet exhaust noise. In *Structure and Mechanisms of Turbulence II* (ed. H. Fiedler), Lecture Notes in Physics, vol. 76, p. 254. Springer-Verlag.

MORRISON, G. L. & MCLAUGHLIN, D. K. 1979 The noise generated by instabilities in low Reynolds number supersonic jets. *J. Sound Vib.* **65**, 177–191.

RIBNER, H. S. 1964 The generation of sound by turbulent jets. *Adv. Appl. Mech.* **VIII**, 103–182. Academic.

RIBNER, H. S. 1981 Perspectives on jet noise. *AIAA J.* **19**, 1513–1526, *Dryden Lecture.*

RICHARZ, W. G. 1983 Length- and time-scales relevant to sound generation in excited jets. *AIAA J.* **21**, 148–149.

SAROHIA, V. & MASSIER, P. F. 1977 Experimental results of large scale structures in jet flows and their relation to jet noise production. *AIAA Paper*-77-1350.

SIDDON, T. E. 1969 Investigation of pressure probe response in unsteady flow. *NASA* SP207.

ZAMAN, K. B. M. Q. 1983 Large-scale coherent structure and far-field jet noise. In *Proc. Fourth Symp. Turb. Shear Flows, Karlsruhe*, 16.23–16.28.

ZAMAN, K. B. M. Q. 1985 Flow-field and near- and far-field of a subsonic jet. *J. Sound Vib.* (Submitted.)

ZAMAN, K. B. M. Q. & HUSSAIN, A. K. M. F. 1980 Vortex pairing in a circular jet under controlled excitation, part 1. General jet response. *J. Fluid Mech.* **101**, 449–491.

ZAMAN, K. B. M. Q. & HUSSAIN, A. K. M. F. 1981 Turbulence suppression in free shear flows by controlled excitation. *J. Fluid Mech.* **103**, 133–160.

ZAMAN, K. B. M. Q. & HUSSAIN, A. K. M. F. 1984 Natural large-scale structures in the axisymmetric mixing layer. *J. Fluid Mech.* **138**, 325–351.

ZAMAN, K. B. M. Q. & YU, J. C. 1985 Power spectral density of subsonic jet noise. *J. Sound Vib.* (To appear.)